REPORT DOCUMENTATION PAGE

Form Approved OMB NO. 0704-0188

1. REPORT DATE (DD-MM-YYYY)	2. REPORT TYPE	3. DATES COVERED (From - To)
19-07-2010	Final Report	1-Jul-2006 - 31-Mar-2010

4. TITLE AND SUBTITLE

Synthesis of Bulk Nanostructured Al Alloys with Ultra-high Strength for Army Applications

5a. CONTRACT NUMBER
W911NF-06-1-0230

5b. GRANT NUMBER

5c. PROGRAM ELEMENT NUMBER
611102

6. AUTHORS

Enrique J. Lavernia

5d. PROJECT NUMBER

5e. TASK NUMBER

5f. WORK UNIT NUMBER

7. PERFORMING ORGANIZATION NAMES AND ADDRESSES

University of California - Davis
Sponsored Programs
118 Everson Hall
Davis, CA 95616 -8671

8. PERFORMING ORGANIZATION REPORT NUMBER

9. SPONSORING/MONITORING AGENCY NAME(S) AND ADDRESS(ES)

U.S. Army Research Office
P.O. Box 12211
Research Triangle Park, NC 27709-2211

10. SPONSOR/MONITOR'S ACRONYM(S)
ARO

11. SPONSOR/MONITOR'S REPORT NUMBER(S)
49554-MS.10

12. DISTRIBUTION AVAILIBILITY STATEMENT

Approved for Public Release; Distribution Unlimited

13. SUPPLEMENTARY NOTES

The views, opinions and/or findings contained in this report are those of the author(s) and should not contrued as an official Department of the Army position, policy or decision, unless so designated by other documentation.

14. ABSTRACT

The objective of this research program was to develop and synthesize new bulk light-weight materials with desirable microstructural features and optimal structural combinations (e.g., nanocrystalline, amorphous, multi-phase) that can endow the material with ultra-high strength for future Army systems. The program spanned the time period from June 1, 2006 to March 31, 2010 and research efforts were devoted to the synthesis and characterization of nanostructured Ti and Mg, and Al nanocomposites (reinforced with amorphous particles), and

15. SUBJECT TERMS

Nanostructured Al alloy, Al nanocomposite, Nanostructured Mg alloy, Nanostructured Ti, Cryomilling, Powder consolidation, Spark plasma sintering, Mechanical performance

16. SECURITY CLASSIFICATION OF:			17. LIMITATION OF ABSTRACT	15. NUMBER OF PAGES	19a. NAME OF RESPONSIBLE PERSON
a. REPORT	b. ABSTRACT	c. THIS PAGE			Enrique Lavernia
UU	UU	UU	UU		19b. TELEPHONE NUMBER: 530-752-4964

Report Title

Synthesis of Bulk Nanostructured Al Alloys with Ultra-high Strength for Army Applications

ABSTRACT

The objective of this research program was to develop and synthesize new bulk light-weight materials with desirable microstructural features and optimal structural combinations (e.g., nanocrystalline, amorphous, multi-phase) that can endow the material with ultra-high strength for future Army systems. The program spanned the time period from June 1, 2006 to March 31, 2010 and research efforts were devoted to the synthesis and characterization of nanostructured Ti and Mg, and Al nanocomposites (reinforced with amorphous particles), and the primary accomplishments are described in this final report.

Bulk Al-Al85Ni10La5 and 5083 Al-Al85Ni10La5 composites were synthesized via different materials processing routes. The microstructural evolution that occurs during the consolidation process (e.g., HIP and extrusion) was characterized using SEM and TEM. The mechanical properties of the consolidated bulk composites were evaluated and the results showed that load transfer played an important role in the observed strength enhancement.

Nanostructured Mg alloy was fabricated using a cryomilling technique followed by consolidations via spark plasma sintering (SPS), and hot isostatic pressing (HIP) and extrusion, respectively. The experimental results showed that cryomilling for 8 hours yields nanostructured Mg agglomerates, approximately 30 micron in size, with an internal average grain size of approximately 40 nm. The SPS'ed Mg AZ80 alloy consisted of a bimodal microstructure with nano-fine and coarse grains. A compressive strength of 546 MPa was measured.

Cryomilled nanocrystalline CP-Ti powders were spark plasma sintered (SPS) in order to study the influence of SPS processing parameters on microstructure evolution and corresponding mechanical behavior. Results were rationalized on the basis of the relevant literature and experimental results, and revealed a strong dependence on SPS parameters. An interesting finding was that the measured high ductility was accompanied by a moderate strength (YS=770 MPa, UTS=840 MPa with ~27% elongation to failure).

List of papers submitted or published that acknowledge ARO support during this reporting period. List the papers, including journal references, in the following categories:

(a) Papers published in peer-reviewed journals (N/A for none)

[1] Z. Zhang, B. Q. Han Y. Zhou, E. J. Lavernia, "Elevated temperature mechanical behavior of bulk nanostructured Al 5083-Al85Ni10La5 composite", Materials Science and Engineering A, Vol. 493, 2008, 221-225.

[2] Z. Zhang, N. Yang, Y. Zhou, E. J. Lavernia, "Nanocrystal formation in gas-atomized amorphous Al85Ni10La5 alloy", Philosophical Magazine, Vol. 88, 2008, 737-753.

[3] Z. Zhang, Y. Zhou, and E. J. Lavernia, "Amorphization and crystallization in Al-Ni-La during mechanical milling", Journal of Alloys and Compounds, Vol. 466, pp. 189-200,2008.

[4] O. Ertorer, T. Topping, Y. Li, W. Moss, and E.J. Lavernia, "Enhanced tensile strength and high ductility in cryomilled commercially pure titanium" Scripta Materialia, Vol. 60, pp. 586-589, 2009.

[5] O. Ertorer, T.D. Topping, Y. Li, Y. Zhao, W. Moss, and E.J. Lavernia, Materials Science Forum Vols. 633-634, p. 459, 2010.

Number of Papers published in peer-reviewed journals: 5.00

(b) Papers published in non-peer-reviewed journals or in conference proceedings (N/A for none)

Number of Papers published in non peer-reviewed journals: 0.00

(c) Presentations

[1] Z. Zhang, T. Topping, Y. Zhou, and E. J. Lavernia, “Mechanical behavior of Al-Al85Ni10La5 in-situ nanocomposites by mechanical milling”, MS&T 2008, October 5-9, Pittsburgh, PA.
[2] Z. Zhang, Y. Zhou, E. J. Lavernia, “Synthesis of Al-Al85Ni10La5 Nanocomposites by Mechanical Milling”, TMS 2008 Annual Meeting and Exhibition, March 9-13, 2008 New Orleans, LA.
[3] Z. Zhang, T. Topping, Y. Zhou, E. J. Lavernia, “Mechanical Behavior of Al-Al85Ni10La5 in situ Nanocomposites by Mechanical Milling”, MS&T 2008, October 5-9, Pittsburgh, PA.
[4] O. Ertorer, T. Topping, Y. Li, W. Moss, E.J. Lavernia "Cryomilled Commercially Pure Titanium with High Strength and Ductility", Poster Presentation, TMS 2009 Annual Meeting and Exhibition, February 15-19, 2009, San Francisco, CA.
[5] O. Ertorer, T. Topping, Y. Li, Y.H. Zhao, W. Moss, E.J. Lavernia "Methods for Improving Ductility in Nanostructured Titanium Prepared via Powder Metallurgical Routes", Oral Presentation, TMS 2010 Annual Meeting and Exhibition, February 14-18, 2010, Seattle, WA.
[6] O. Ertorer, H. Wen, Y. Li, Y.H. Zhao, R.Z. Valiev, E.J. Lavernia "Nanostructured Commercially Pure Titanium Prepared via Cryomilling and High Pressure Torsion (HPT)", Poster presentation, TMS 2010 Annual Meeting and Exhibition, February 14-18, 2010, Seattle, WA.

Number of Presentations: 6.00

Non Peer-Reviewed Conference Proceeding publications (other than abstracts):

Number of Non Peer-Reviewed Conference Proceeding publications (other than abstracts): 0

Peer-Reviewed Conference Proceeding publications (other than abstracts):

Number of Peer-Reviewed Conference Proceeding publications (other than abstracts): 0

(d) Manuscripts

[1] Osman Ertorer, Troy D. Topping, Ying Li, Wes Moss, Enrique J. Lavernia, “Nanostructured Ti consolidated via spark plasma sintering”, submitted to Acta Materialia, March 2010.
[2] Baolong Zheng, Osman Ertorer, Ying Li, Yizhang Zhou, Chi Y.A. Tsao, and Enrique J. Lavernia, “High strength, nano-structured Mg-Al-Zn Alloy”, submitted to Materials Science and Engineering –A, June 2010.

Number of Manuscripts: 2.00

Patents Submitted

Patents Awarded

Graduate Students

NAME	PERCENT_SUPPORTED
Osman Ertorer	0.49
FTE Equivalent:	**0.49**
Total Number:	**1**

Names of Post Doctorates

NAME	PERCENT_SUPPORTED
Baolong Zheng	0.25
Zhihui Zhang	0.30
Ying Li	0.05
FTE Equivalent:	**0.60**
Total Number:	**3**

Names of Faculty Supported

NAME	PERCENT_SUPPORTED	National Academy Member
Enrique J. Lavernia	0.05	No
FTE Equivalent:	**0.05**	
Total Number:	**1**	

Names of Under Graduate students supported

NAME	PERCENT_SUPPORTED
FTE Equivalent:	
Total Number:	

Student Metrics

This section only applies to graduating undergraduates supported by this agreement in this reporting period

The number of undergraduates funded by this agreement who graduated during this period:	0.00
The number of undergraduates funded by this agreement who graduated during this period with a degree in science, mathematics, engineering, or technology fields:	0.00
The number of undergraduates funded by your agreement who graduated during this period and will continue to pursue a graduate or Ph.D. degree in science, mathematics, engineering, or technology fields:	0.00
Number of graduating undergraduates who achieved a 3.5 GPA to 4.0 (4.0 max scale):	0.00
Number of graduating undergraduates funded by a DoD funded Center of Excellence grant for Education, Research and Engineering:	0.00
The number of undergraduates funded by your agreement who graduated during this period and intend to work for the Department of Defense	0.00
The number of undergraduates funded by your agreement who graduated during this period and will receive scholarships or fellowships for further studies in science, mathematics, engineering or technology fields:	0.00

Names of Personnel receiving masters degrees

NAME
Total Number:

Names of personnel receiving PHDs

NAME
Zhihui Zhang
Total Number: 1

Names of other research staff

NAME	PERCENT SUPPORTED	
Yizhang Zhou	0.05	No
FTE Equivalent:	**0.05**	
Total Number:	**1**	

Sub Contractors (DD882)

Inventions (DD882)

REPORT DOCUMENTATION PAGE

Form Approved
OMB NO. 0704-0188

1. AGENCY USE ONLY (Leave Blank)	2. REPORT DATE	3. REPORT TYPE AND DATES COVERED Final Technical Report June 1, 2006 – March 31, 2010

4. TITLE AND SUBTITLE
Synthesis of Bulk Nanostructured Al Alloys with Ultra-high Strength for Army Applications

5. FUNDING NUMBERS
W911NF-06-1-0230

6. AUTHOR(S)
E.J. Lavernia

7. PERFORMING ORGANIZATION NAME(S) AND ADDRESS(ES)
University of California, Davis
One shields Ave
Davis, CA 95616

8. PERFORMING ORGANIZATION REPORT NUMBER

9. SPONSORING / MONITORING AGENCY NAME(S) AND ADDRESS(ES)
U. S. Army Research Office
P.O. Box 12211
Research Triangle Park, NC 27709-2211

10. SPONSORING / MONITORING AGENCY REPORT NUMBER

11. SUPPLEMENTARY NOTES
The views, opinions and/or findings contained in this report are those of the author(s) and should not be construed as an official Department of the Army position, policy or decision, unless so designated by other documentation.

12 a. DISTRIBUTION / AVAILABILITY STATEMENT
Approved for public release; distribution unlimited.

12 b. DISTRIBUTION CODE

13. ABSTRACT (Maximum 200 words)

The objective of this research program was to develop and synthesize new bulk light-weight materials with desirable microstructural features and optimal structural combinations (e.g., nanocrystalline, amorphous, multi-phase) that can endow the material with ultra-high strength for future Army systems. The program spanned the time period from June 1, 2006 to March 31, 2010 and research efforts were devoted to the synthesis and characterization of nanostructured Ti and Mg, and Al nanocomposites (reinforced with amorphous particles), and the primary accomplishments are described in this final report.

Bulk Al-$Al_{85}Ni_{10}La_5$ and 5083 Al-$Al_{85}Ni_{10}La_5$ composites were synthesized via different materials processing routes. The microstructural evolution that occurs during the consolidation process (e.g., HIP and extrusion) was characterized using SEM and TEM. The mechanical properties of the consolidated bulk composites were evaluated and the results showed that load transfer played an important role in the observed strength enhancement.

Nanostructured Mg alloy was fabricated using a cryomilling technique followed by consolidations via spark plasma sintering (SPS), and hot isostatic pressing (HIP) and extrusion, respectively. The experimental results showed that cryomilling for 8 hours yields nanostructured Mg agglomerates, approximately 30 μm in size, with an internal average grain size of approximately 40 nm. The SPS'ed Mg AZ80 alloy consisted of a bimodal microstructure with nano-fine and coarse grains. A compressive strength of 546 MPa was measured.

Cryomilled nanocrystalline CP-Ti powders were spark plasma sintered (SPS) in order to study the influence of SPS processing parameters on microstructure evolution and corresponding mechanical behavior. Results were rationalized on the basis of the relevant literature and experimental results, and revealed a strong dependence on SPS parameters. An interesting finding was that the measured high ductility was accompanied by a moderate strength (YS=770 MPa, UTS=840 MPa with ~27% elongation to failure).

14. SUBJECT TERMS	15. NUMBER OF PAGES
Nanostructured Al alloy, Al nanocomposite, Nanostructured Mg alloy, Nanostructured Ti, Cryomilling, Powder consolidation, Spark plasma sintering, Mechanical performance	16. PRICE CODE

17. SECURITY CLASSIFICATION OR REPORT	18. SECURITY CLASSIFICATION ON THIS PAGE	19. SECURITY CLASSIFICATION OF ABSTRACT	20. LIMITATION OF ABSTRACT
UNCLASSIFIED	**UNCLASSIFIED**	**UNCLASSIFIED**	**UL**

REPORT DOCUMENTATION PAGE (SF298)
(Continuation Sheet)

1. List of Publications and Presentations

[1] Z. Zhang, B. Q. Han Y. Zhou, E. J. Lavernia, "Elevated temperature mechanical behavior of bulk nanostructured Al 5083-$Al_{85}Ni_{10}La_5$ composite", *Materials Science and Engineering A*, Vol. 493, 2008, 221-225.

[2] Z. Zhang, N. Yang, Y. Zhou, E. J. Lavernia, "Nanocrystal formation in gas-atomized amorphous $Al_{85}Ni_{10}La_5$ alloy", *Philosophical Magazine*, Vol. 88, 2008, 737-753.

[3] Z. Zhang, Y. Zhou, and E. J. Lavernia, "Amorphization and crystallization in Al-Ni-La during mechanical milling", *Journal of Alloys and Compounds*, Vol. 466, pp. 189-200,2008.

[4] Z. Zhang, T. Topping, Y. Zhou, and E. J. Lavernia, "Mechanical behavior of Al-$Al_{85}Ni_{10}La_5$ in-situ nanocomposites by mechanical milling", MS&T 2008, October 5-9, Pittsburgh, PA.

[5] O. Ertorer, T. Topping, Y. Li, W. Moss, and E.J. Lavernia, "Enhanced tensile strength and high ductility in cryomilled commercially pure titanium" Scripta Materialia, Vol. 60, pp. 586-589, 2009.

[6] O. Ertorer, T.D. Topping, Y. Li, Y. Zhao, W. Moss, and E.J. Lavernia, Materials Science Forum Vols. 633-634, p. 459, 2010.

[7] Baolong Zheng, Osman Ertorer, Ying Li, Yizhang Zhou, Chi Y.A. Tsao, and Enrique J. Lavernia, "High strength, nano-structured Mg-Al-Zn Alloy", submitted to Materials Science and Engineering –A, June 2010.

[8] Osman Ertorer, Troy D. Topping, Ying Li, Wes Moss, Enrique J. Lavernia, "Nanostructured Ti consolidated via spark plasma sintering", submitted to Acta Materialia, March 2010.

[9] Z. Zhang, Y. Zhou, E. J. Lavernia, "Synthesis of Al-$Al_{85}Ni_{10}La_5$ Nanocomposites by Mechanical Milling", TMS 2008 Annual Meeting and Exhibition, March 9-13, 2008 New Orleans, LA.

[10] Z. Zhang, T. Topping, Y. Zhou, E. J. Lavernia, "Mechanical Behavior of Al-$Al_{85}Ni_{10}La_5$ in situ Nanocomposites by Mechanical Milling", MS&T 2008, October 5-9, Pittsburgh, PA.

[11] O. Ertorer, T. Topping, Y. Li, W. Moss, E.J. Lavernia "Cryomilled Commercially Pure Titanium with High Strength and Ductility", Poster Presentation, TMS 2009 Annual Meeting and Exhibition, February 15-19, 2009, San Francisco, CA.

[12] O. Ertorer, T. Topping, Y. Li, Y.H. Zhao, W. Moss, E.J. Lavernia "Methods for Improving Ductility in Nanostructured Titanium Prepared via Powder Metallurgical Routes", Oral Presentation, TMS 2010 Annual Meeting and Exhibition, February 14-18, 2010, Seattle, WA.

[13] O. Ertorer, H. Wen, Y. Li, Y.H. Zhao, R.Z. Valiev, E.J. Lavernia "Nanostructured Commercially Pure Titanium Prepared via Cryomilling and High Pressure Torsion (HPT)", Poster presentation, TMS 2010 Annual Meeting and Exhibition, February 14-18, 2010, Seattle, WA.

[14] Baolong Zheng, Dongming Liu, Yizhang Zhou, and Enrique J. Lavernia, "Bimodal microstructure formation during SPSing nanostructure alloys", In preparation.

[15] Zhihui Zhang, Ying Li, Troy Topping, Yizhang Zhou, Enrique J Lavernia, "Mechanical properties of ultrafine grained Al-Al85Ni10La5 composites", In preparation.

2. Scientific Personnel

Mr. Osman Ertorer, PhD Candidate
Mr. Troy Topping, PhD Candidate
Dr. Baolong Zheng, Post-doctoral Researcher
Dr. Ying Li, Post-doctoral Researcher
Dr. Zhihui Zhang, Post-doctoral Researcher
Dr. Yizhang Zhou, Associate Researcher

3. Scientific Progress and Accomplishments

The technical objectives of this research program were to develop and synthesize new bulk light-weight materials with desirable microstructural features and optimal structural combinations (e.g., nanocrystalline, amorphous, multi-phase) that endow the material with ultra-high strength for future Army systems. The research work involved the following two aspects: first, to establish a fundamental relationship between synthesis, microstructure and mechanical behavior of these novel classes of materials; second, to enhance our fundamental understanding of the deformation mechanisms of bulk composite materials and multi-phase alloys that own a characteristic dimension falling in the nanometer scale. This report covers the research activities

made during the period from June 1, 2006 to March 31, 2010. The major accomplishments in this project are described as follows.

3.1 Al-$Al_{85}Ni_{10}La_5$ Composite

3.1.1 Synthesis and analysis of AlNiLa amorphous powder

An inert gas atomization technique was applied to produce the amorphous AlNiLa alloy powder of interest that can be used as a reinforcement phase in synthesis of Al/Al alloy based composites via mechanical milling processing route. In order to further study the phase transformation reactions that occur in $Al_{85}Ni_{10}La_5$ alloy during mechanical milling, fully and partially amorphous AlNiLa ribbons (comprised of fcc-Al, Al_3Ni, $Al_{11}La_3$ and amorphous phases) as starting materials were selected for this purpose. X-ray diffraction (XRD) analysis and transmission electron microscopy (TEM) studies showed that the Al_3Ni phase crystallized whereas the $Al_{11}La_3$ phase amorphized during mechanical milling. Differential scanning calorimetry (DSC) analysis revealed that the difference in the structural stability of the Al_3Ni and $Al_{11}La_3$ phases are related to the chemical short-range order of the solute atoms in the amorphous phase. Additional information of the study can be found in the previously submitted annual technical reports.

3.1.2 Synthesis and microstructural analysis of AlNiLa reinforced Al and Al alloy composites

Two materials processing routes were used to fabricate bulk AlNiLa reinforced Al and Al alloy composites. These include: (1) direct mixing of as-atomized amorphous $Al_{85}Ni_{10}La_5$ powder with cryomilled Al powder followed by consolidation, and (2) cryomilling of a powder mixture of commercial purity Al and amorphous $Al_{85}Ni_{10}La_5$ followed by consolidation.

Figure 1 shows the optical microscope (OM) micrographs of an amorphous phase reinforced nanostructured 5083 Al alloy which was fabricated via a powder mixture of amorphous $Al_{85}Ni_{10}La_5$ powders and cryomilled 5083 Al powders followed by a conventional consolidation process of a cold isostatic press (CIP) and extrusion, herein designated as *micro-nano-composites*. It can be seen that the $Al_{85}Ni_{10}La_5$ powders are uniformly distributed in 5083 Al matrix (Figure 1a). The amorphous $Al_{85}Ni_{10}La_5$ powders are homogeneously crystallized during the extrusion process and the crystallized phases have a size of approximately 100 nm (Figure 1b and 1c).

Figure 2 shows the TEM images of bulk amorphous phase reinforced nanostructured Al in which amorphous $Al_{85}Ni_{10}La_5$ powder and as-atomized commercial purity Al powder was blended, cryomilled together and then consolidated into bulk samples via degassing, HIP and extrusion, herein designated as *nano-nano-composites*. TEM images taken from HIP'ed, and extruded samples, respectively, indicated that the grain size of Al matrix in the HIP'ed sample is around 100-200 nm (Figure 2a) and following extrusion, the grain size of the Al matrix is around 200-300 nm (Figure 2b). Since the extrusion temperature (300 ^oC) is lower than that of the HIPping temperature (400 ^oC), the TEM results suggested that the deformation during extrusion induced grain growth.

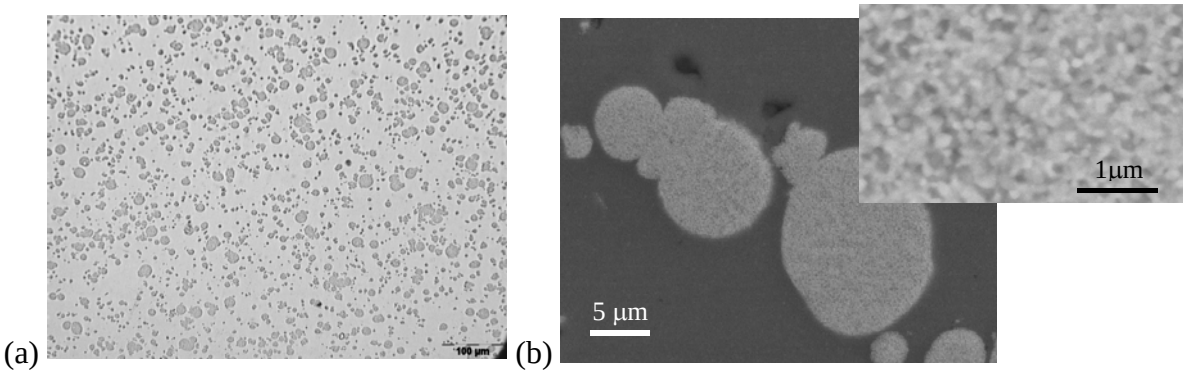

Figure 1. (a) OM image showing homogeneous distribution of the $Al_{85}Ni_{10}La_5$ particles (20% in 5083 Al matrix); (b) BSE images of the $Al_{85}Ni_{10}La_5$ particles.

(a) 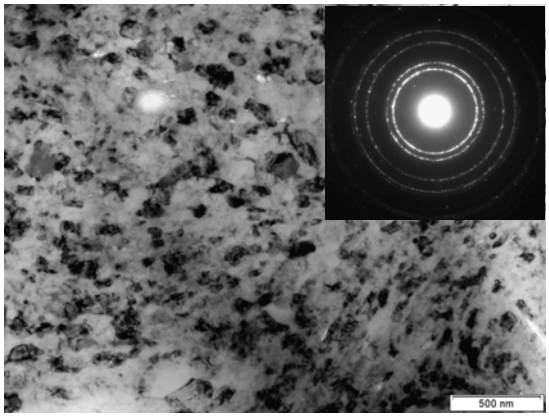 (b) 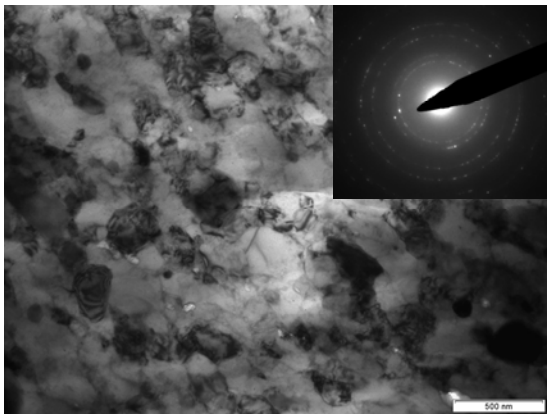

Figure 2. TEM images of bulk Al-5%$Al_{85}Ni_{10}La_5$ composite: (a) HIP'ed sample (Al matrix), (b) Extruded sample (Al matrix).

A direct cryomilling of a powder mixture of commercial purity Al and amorphous $Al_{85}Ni_{10}La_5$ led to a significant refinement in particle size of the $Al_{85}Ni_{10}La_5$ powder in the nano-nano composites, as compared to the micro-nano composites. In the nano-nano-composites, the $Al_{85}Ni_{10}La_5$ reinforcement showed a large aspect ratio of approximately 20. $Al_{85}Ni_{10}La_5$ particle size refinement was achieved during cryomilling, as shown in the as-HIP'ed sample in Figure 3a, and the aspect ratio was further significantly enhanced during extrusion, as shown in Figures 3b, 3c and 3d. Fiber-like $Al_{85}Ni_{10}La_5$ reinforcement phase was generated in the nano-nano-composites. This is in contrast to the micro-nano-composites, where limited aspect ratio was observed with increasing the volume fraction to 20% (Figures 4). Figure 5 shows the effect of cryomilling on the reinforcement aspect ratio.

(a) 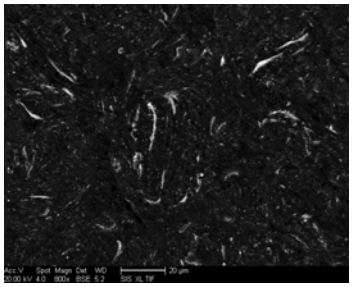 (b) 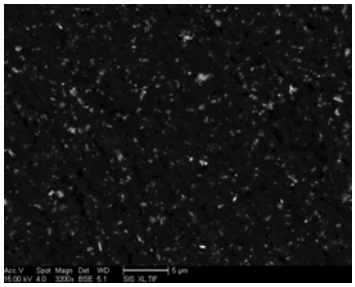 (c) 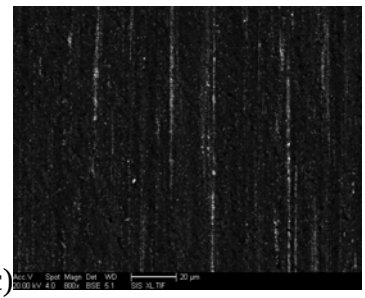

Figure 3. SEM BSE images showing distribution of $Al_{85}Ni_{10}La_5$ reinforcement (nano-nano-composites). (a) HIP'ed sample. (b) Extruded sample in transverse direction. (c) Extruded sample in longitudinal direction.

(a) 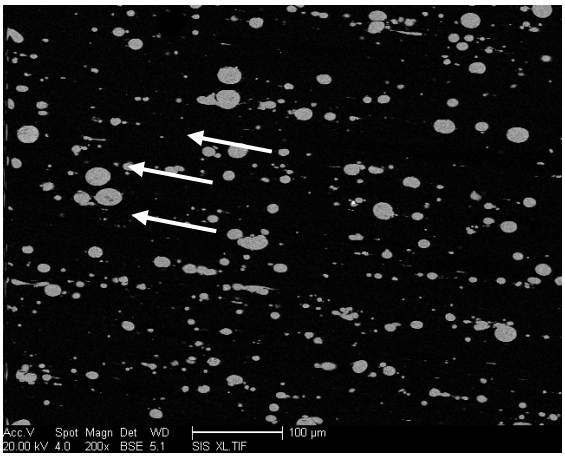 (b) 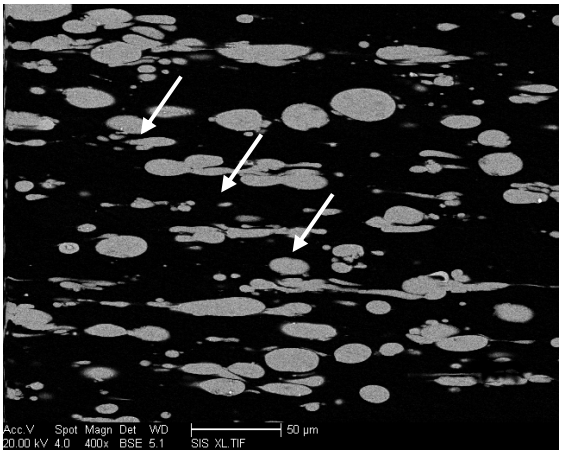

Figure 4. SEM BSE images showing distribution of $Al_{85}Ni_{10}La_5$ in extruded samples (micro-nano-composites). (a) 10% $Al_{85}Ni_{10}La_5$. (b) 20% $Al_{85}Ni_{10}La_5$.

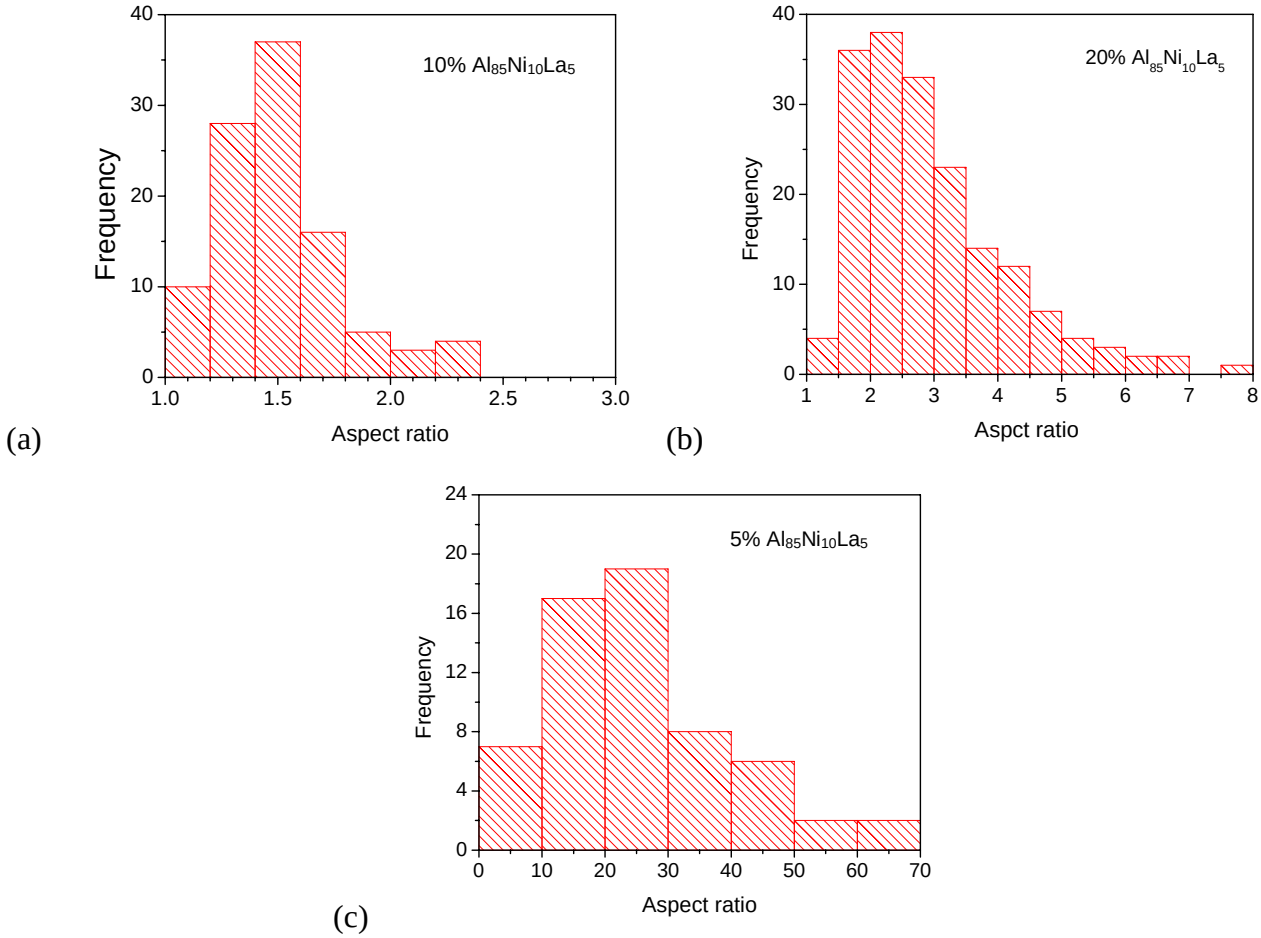

Figure 5. The effect of cryomilling on the reinforcement aspect ratio. (a and b) The $Al_{85}Ni_{10}La_5$ reinforcement was blended following cryomilling. (c) The $Al_{85}Ni_{10}La_5$ reinforcement was blended prior to cryomilling.

3.1.3 Mechanical Properties of Al-$Al_{85}Ni_{10}La_5$ Composite

The reinforcement effect of the $Al_{85}Ni_{10}La_5$ phase on the mechanical properties of the composites was studied. Compressive tests showed that the bulk micron-nano composite sample with 20 vol.% $Al_{85}Ni_{10}La_5$ and 80 vol.% 5083Al exhibited a strength higher than 1000 MPa, whereas the bulk micron-nano composite sample with 10 vol.% $Al_{85}Ni_{10}La_5$ and 90 vol.% 5083Al showed a strength higher than 800 MPa (see Figure 6). For comparison purposes, a stress-strain curve of a conventional coarse-grained 5083 Al was also included.

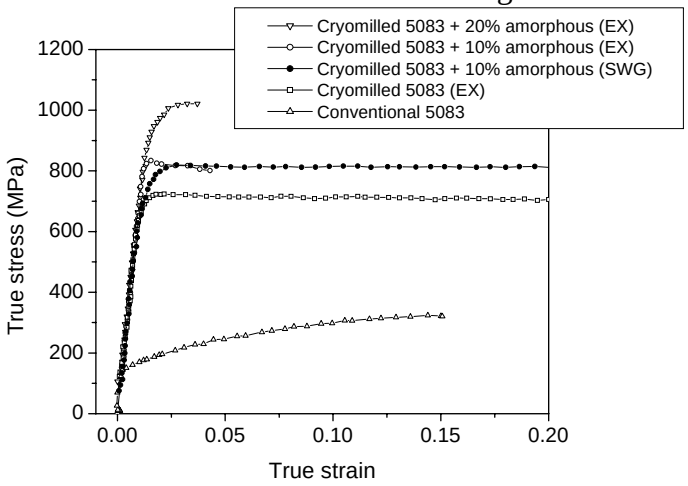

Figure 6. Compressive stress vs. strain curves of cryomilled 5083 Al mixed with 0%, 10% and 20% amorphous $Al_{85}Ni_{10}La_5$ particle. Room temperature.

Compressive and tensile tests of the bulk nano-nano composites were carried out at room temperature and the results are shown in Figure 7. It is very promising that the yield strength (in compression) of nano-nano Al+5vol.% $Al_{85}Ni_{10}La_5$ composite reached 550 MPa, whereas the bulk sample 100% cryomilled Al showed a yield strength of approximately 350 MPa. For comparison purposes, a stress-strain curve of a conventional coarse-grained Al is also included.

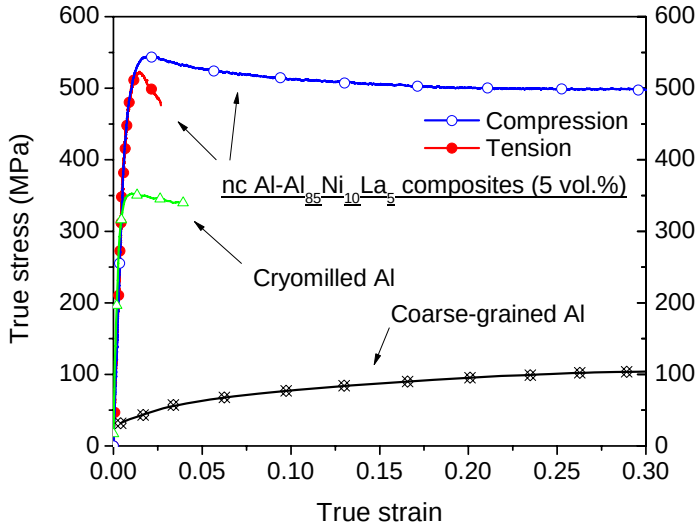

Figure 7. Compressive and tensile stress vs. strain curves of cryomilled Al, and nano-nano Al+5vol.% $Al_{85}Ni_{10}La_5$ composite. Room temperature.

3.2 Nanostructured Mg Alloy

The mechanical behavior and microstructure of nanocrystalline (nc) Mg AZ80 alloy, synthesized via a cryomilling and spark plasma sintering (SPS) approach is reported and discussed. The effects of cryomilling processing on chemistry, particle morphology, and microstructure of the Mg alloy powder are also described and discussed.

3.2.1. Cryomilling of Mg AZ80 Powder

The starting material used in this study was a gas atomized Mg AZ80 powder (7.83wt.% Al, 0.47wt.% Zn, and 0.16wt.% Mn). The as-received Mg AZ80 powder used for cryomilling had an average particle size of 55 μm, distributed in the range of 10 to 106 μm with spherical morphology. Due to a strong affiliation of Mg to nitrogen, the cryogenic milling experiment was performed on a modified 1-S Szegvari-type attritor with liquid argon at temperatures 92 ± 5 K. The Mg powders were cryomilled for 8 hours with a ball-to-powder ratio (BPR) of 60:1 (wt/wt) and an impeller rotation speed of 180 rpm. The process control agent (PCA) was not used in the cryomilling run as the powders did not agglomerate in the liquid Ar media. At the end of the cryomilling runs, the powders were discharged into a closed transfer can, which was then handled in an Ar atmosphere glove box.

(a) 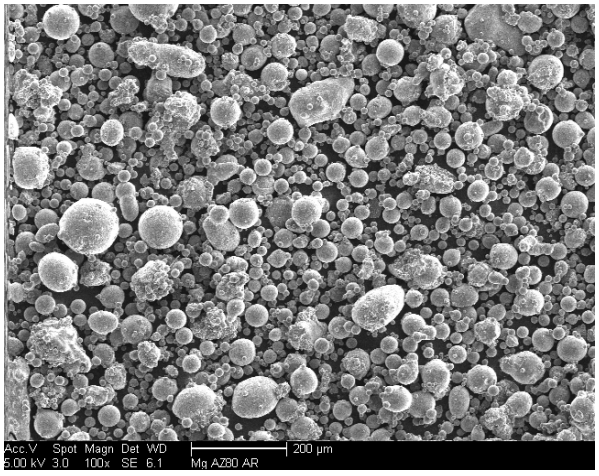

(b) 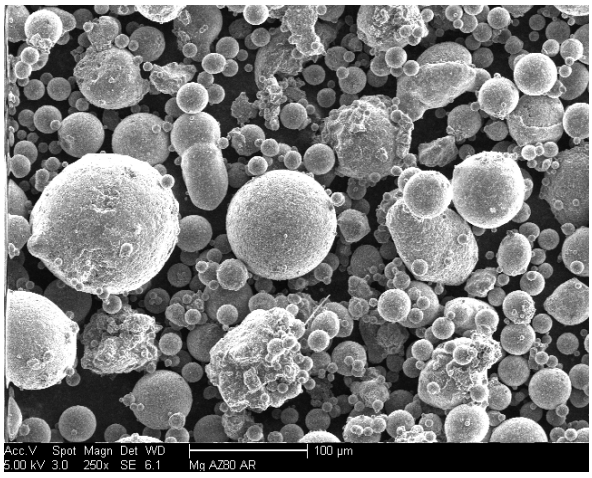

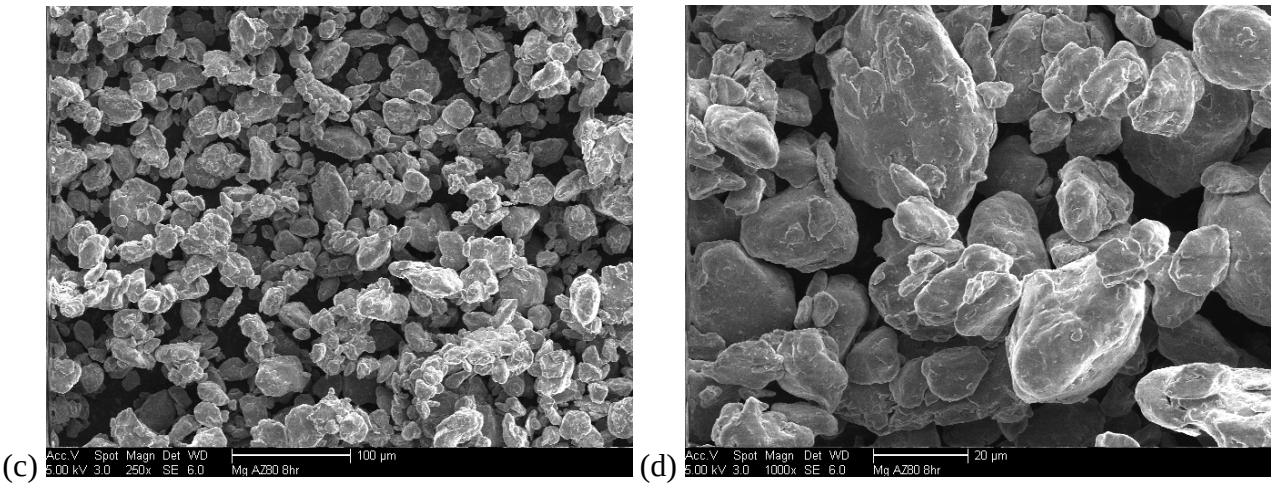

(c) (d)

Figure 8. SEM micrographs showing the morphology of: (a) & (b) as-received gas atomized Mg AZ80 powder and (c) & (d) as-cryomilled Mg powder using liquid argon.

3.2.2 Microstructural Analysis of Cryomilled Mg AZ80 Powder

The cryomilled Mg powders were analyzed using transmission electron microscopy (TEM). Figure 9 shows the TEM micrographs and selected-area diffraction (SAD) pattern of the nanostructured Mg powder after cryomilling of 8 hrs. A statistic grain size range from 10 to 90 nm and an average grain size of 41.2 nm for an 8-hour cryomilled Mg AZ80 powder were obtained from the TEM images. It is interesting to note that some deformation twins were observed as indicated by the arrow in Figure 9(b). As shown in Figure 9(c), the SAD pattern of the Mg grains shows a ring pattern, indicating that the individual grains are in nanoscale size and separated by high-angle grain boundaries and have a random orientation with neighboring grains. The corresponding histogram of the grain size distributions of cryomilled Mg AZ80 powder is given in Figure 9(d). The grain size was found normally distributed and mostly concentrated around 40 nm. Although more than 70% of the grains were in the size range of 20–60 nm, some grains in the coarse regions were as large as 150 nm. Overall, the number-based mean grain size of the as-cryomilled Mg powder was 41.2 nm.

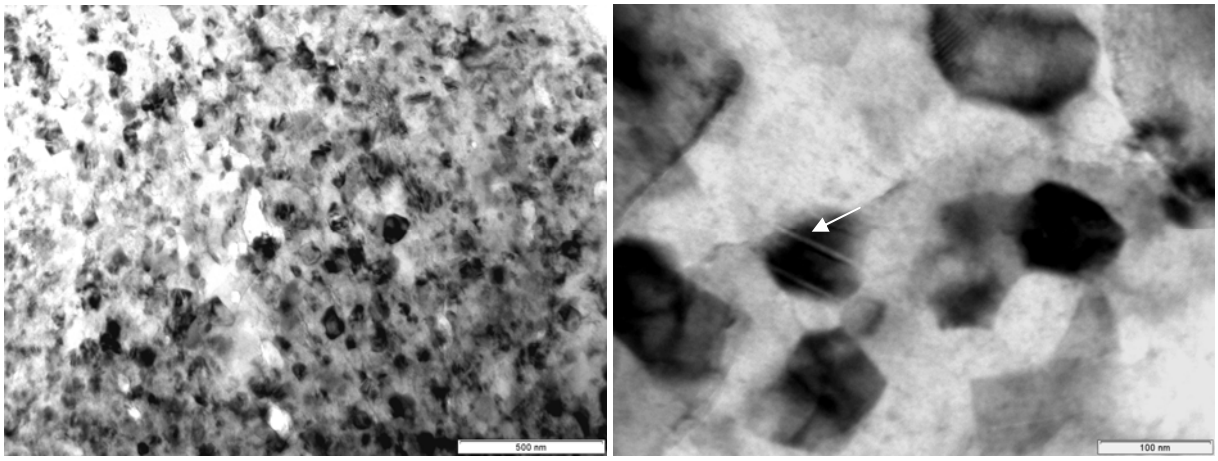

(a) (b)

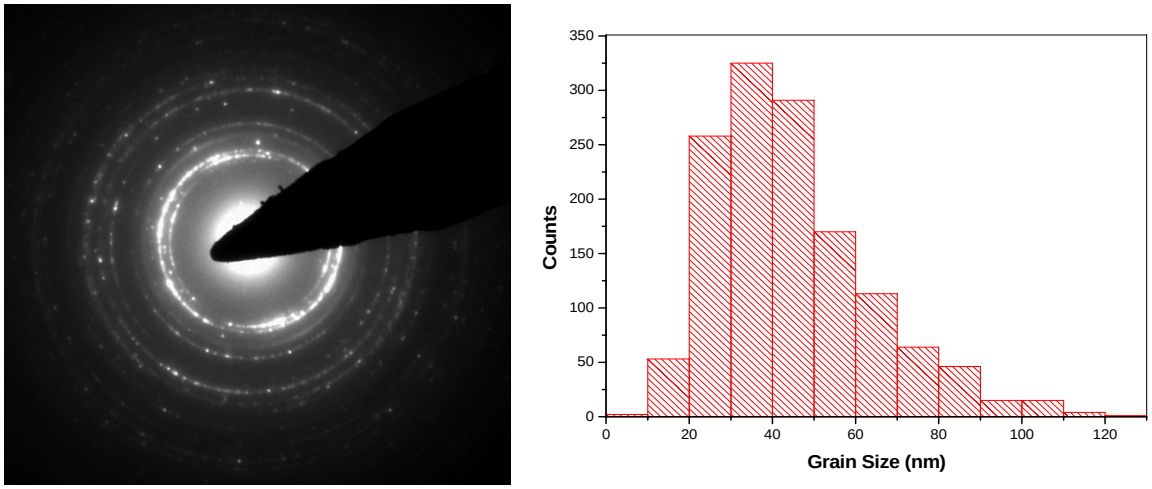

(c) (d)

Figure 9. TEM micrograph of cryomilled Mg AZ80 powders: (a, b) bright-filed image of Mg powder after an 8 hour milling, and (c) its correspondent SAED, and (d) histograms of grain size distribution of cryomilled nanostructured Mg AZ80 powders.

3.2.3 SPS Sintering of Cryomilled Mg Powder

Bulk nanostructured Mg AZ80 alloy samples were fabricated via SPS. Cryomilled powders were consolidated by an SPS-825S DR.SINTER apparatus (SPS Syntex Inc., Japan) under a vacuum condition (lower than 6 Pa). Prior to SPS processing the cryomilled powders were loaded in a graphite die (20 mm diameter) in an Ar glove box to avoid further oxidation of the Mg powder. SPS was performed at different temperatures with 3 minutes of holding time while a heating rate of 120^{o}C/min and a sintering pressure of 100 MPa were used. The purpose of using different sintering temperatures was to investigate its influence on density and mechanical behavior. Figure 10 shows the variation of displacement of graphite die punch units as a function of heating temperature for different sintering temperature and powders. The 1st shrinking regime occurred with increasing temperature while the applied pressure of 80 MPa remained constant. The 2nd shrinking regime occurred with increasing pressure up to 100 MPa while the heating temperature was kept constant.

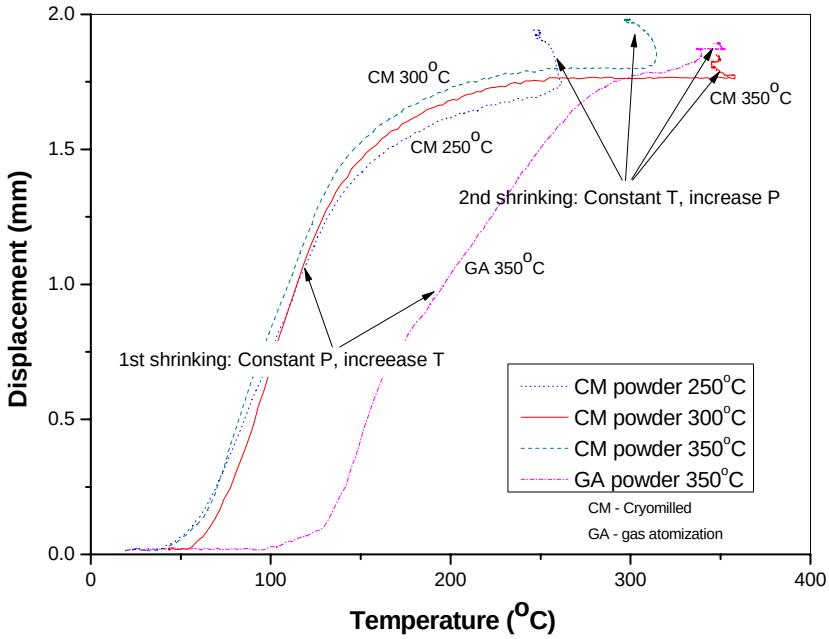

Figure 10. Displacement variation of die punch as a function of heating temperature.

3.2.4 Microstructural Analysis of SPS'ed Bulk Mg

Figure 11 shows the typical TEM micrographs and corresponding selected area electron diffraction (SAED) pattern for the SPS'ed Mg samples, with an observation of bimodal grain structure. In the case of the sample SPS'ed at 350^{o}C, the mean grain size of the fine grain (FG) matrix is measured to be approximately 68.9 nm, which is slightly larger than that of the as-cryomilled Mg powder, presumably suggesting limited grain growth. In comparison, the mean grain size of the coarse grained (CG) region (total 5% in vol.) at the interfaces of particles is measured to be 495.3 nm. The corresponding histograms for the grain size distributions of SPS'ed Mg AZ80 materials are shown in Figure 12. The grains at the particle interfaces appear to have experienced more coarsening when compared to grains in the interior of the particles, leading to the observed bimodal nanostructure. Inside of the coarse grain regions, nano-sized $Mg_{17}Al_{12}$ precipitates (~ 30 nm) were observed. These are illustrated with arrows in Figure 13(a). Energy Dispersive X-ray Spectroscopy (EDX) quantitative analysis, in combination with TEM, was used to measure the relative amounts of elements in precipitated particles. The results, as shown in Figure 13(b), indicate that the precipitated particles contain more Al than that of matrix, which implies that the precipitated particles are possibly $Mg_{17}Al_{12}$ intermetallic phase, based on phase diagram considerations. The relative concentrations of Mn and Zn are also higher around the precipitated particles than that in the matrix.

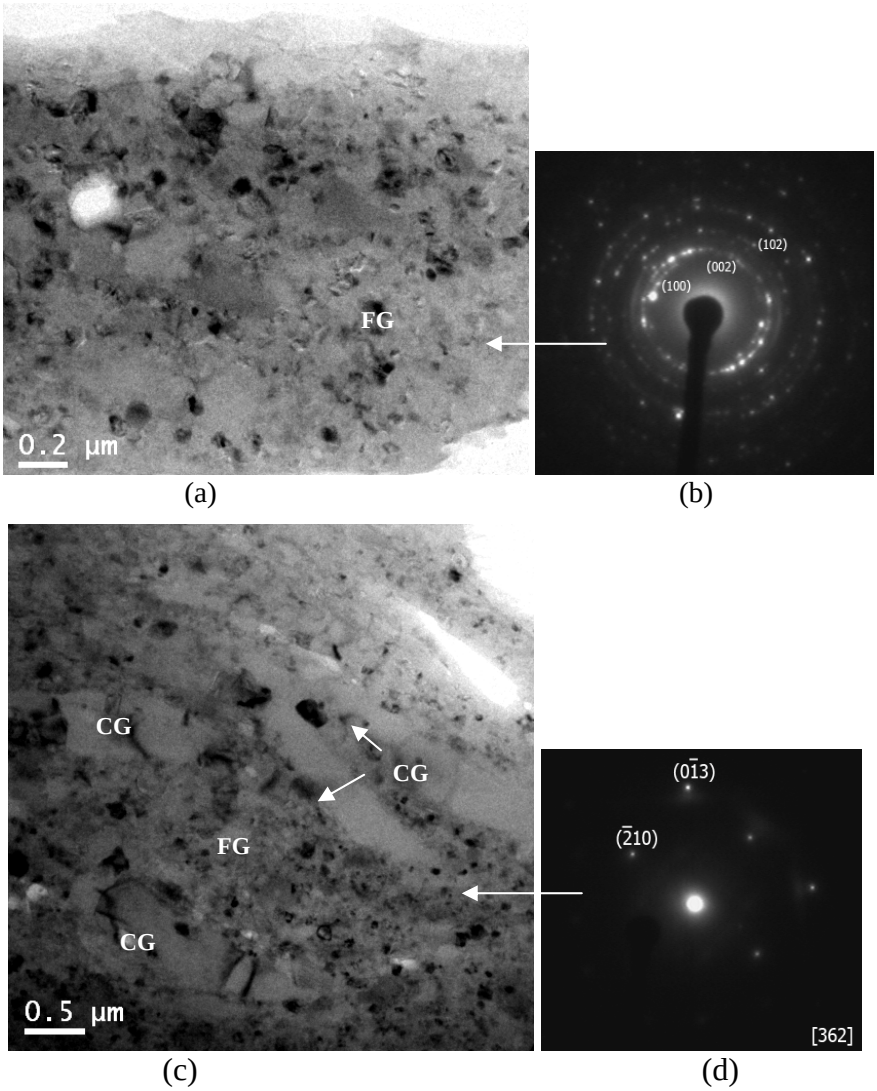

Figure 11. TEM micrograph of SPSed Mg AZ80 bulks: bright-filed image and its correspondent SAD.

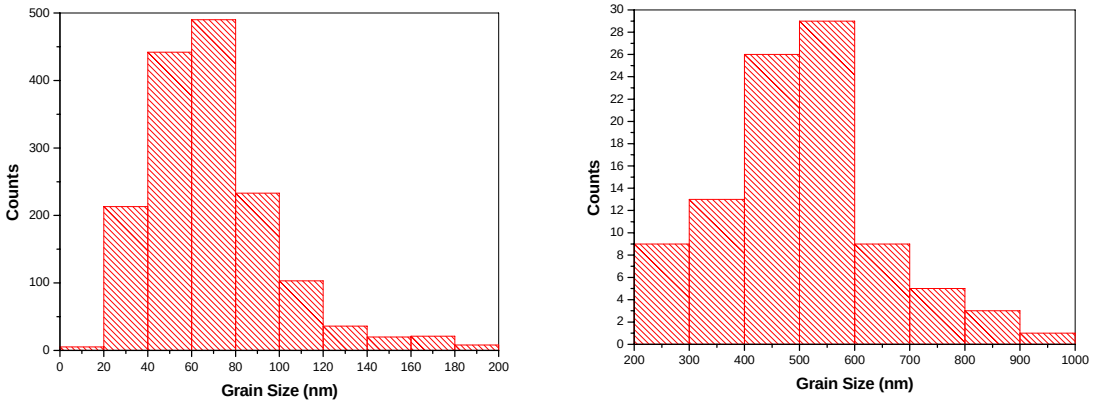

(a) (b)

Figure 12. Histogram of grain size distribution of SPSed Mg AZ80 in (a) fine and (b) coarse grain area.

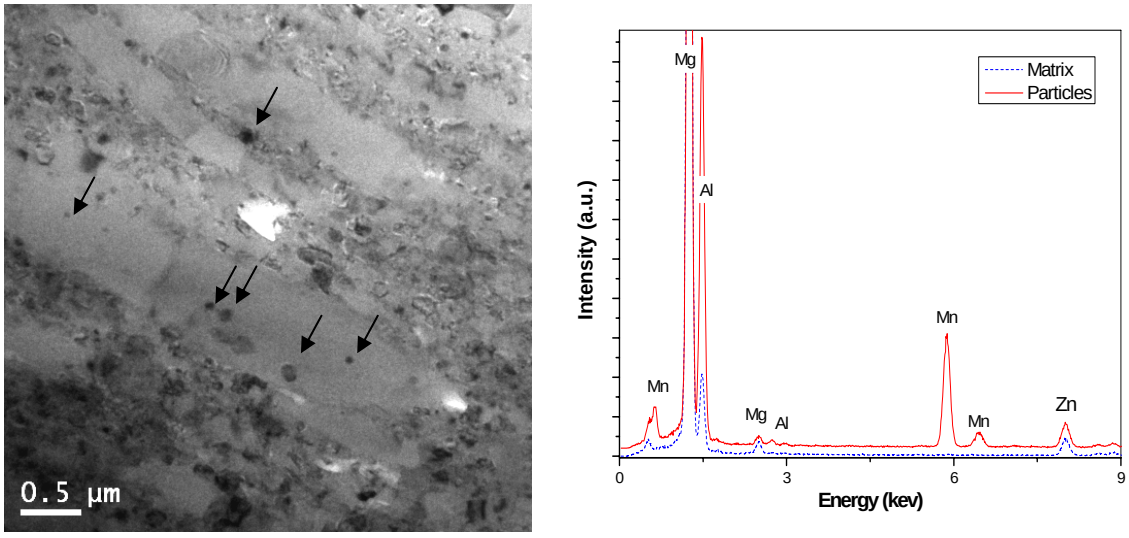

(a) (b)

Figure 13. TEM micrograph of SPSed Mg AZ80 bulks showing precipitated particles in coarse grains.

3.2.5 Mechanical Properties of Bulk Nanostructured Mg

Room temperature compression and microhardness studies were conducted to provide insight into the mechanical behavior of cryomilled, SPS'ed MgAZ80 samples. Figure 14 shows the variation of microhardness for SPS'ed samples fabricated at different temperatures. The microhardness of the SPS'ed samples using cryomilled powder is twice as high as that of the SPS'ed material using as-atomized powder, and moreover, it increases with increasing SPS sintering temperature and a concomitant increase in density. The maximum measured microhardness was 146 HV, which is significantly higher than the values for conventional Mg alloys. Figure 15 shows the compression stress-strain curves of the SPS'ed samples. The measured highest ultimate strength for SPS'ed MgAZ80 (using cryomilled powder) is 545.9 MPa with 4.2% strain at failure. The strength values measured for SPS samples increase with increasing sintering temperature. Despite the fact that temperature increase facilitates grain growth, clearly the extent of densification in this temperature range plays a more important role in strengthening.

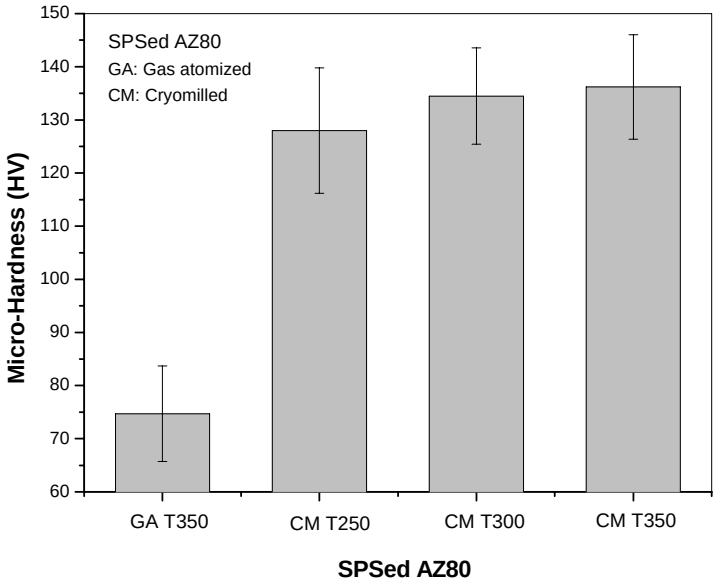

Figure 14. Variation of microhardness measured with different SPS sintering temperature.

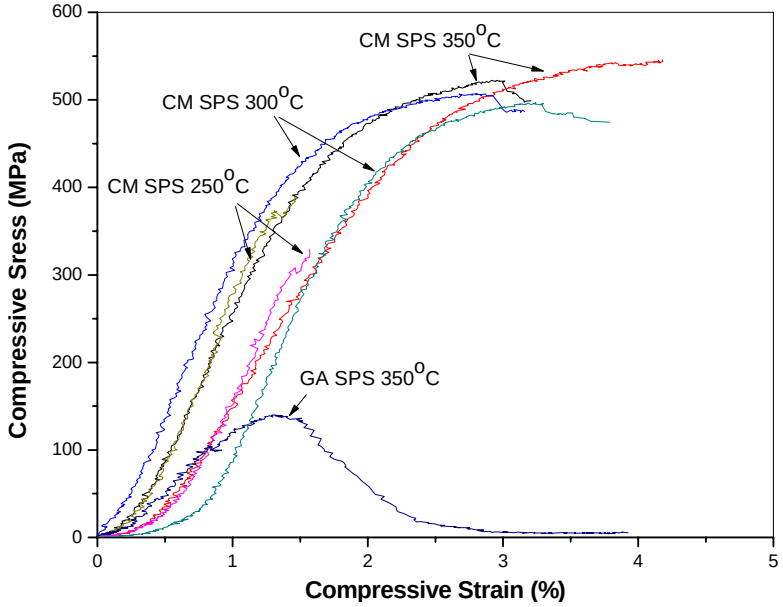

Figure 15. Compressive properties of SPS'ed Mg AZ80 with cryomilled powder.

3.3 Nanostructured Ti Alloys

Nanostructured Ti and Ti alloys were fabricated via cryomilling followed by conventional consolidation including HIP and Forge and Spark Plasma Sintering (SPS), respectively. In this final report, the results of nanostructure CP-Ti synthesized via SPS are described.

3.3.1 Cryomilling

CP-Ti (Grade-II) powders with an average particle size of 55 μm and a chemical composition (in wt.%) of 0.19% O, 0.0017% N, 0.003% C and 0.013% Fe were used as starting materials for the cryomilling experiments. A 1 kg batch of powders was cryomilled for 8 hrs in a liquid argon environment (92 ± 5 K) using a modified Union Process 1-S Szegvari type attritor (impeller rotation speed of 180 rpm), a stainless steel tank, and 30 kg of stainless steel balls. Carbon black (C, 99.9+%, acetylene) (0.4 wt.%) was used as a process control agent (PCA) to improve powder yield. Elemental chemical analyses of both cryomilled powders and SPS processed

bulk samples for O, C, N, H and Fe were carried out by a commercial laboratory. The average grain size of the 8 hrs cryomilled CP-Ti powders was calculated to be 19 nm from analysis of XRD peak broadening data.

3.3.2 Spark Plasma Sintering

The as-processed cryomilled powders were blended with micron sized, as-received powders (70% cryomilled + 30% as-received, wt/wt) using a V-shape blender for 10 hrs in an argon environment. The blended powders were degassed in a closed stainless steel can under vacuum (~10^{-3} Pa) at 350 °C to eliminate moisture and other volatile species. The degassed powders were then stored in an argon glove box until SPS processing to minimize possible atmospheric contamination.

SPS experiments were carried out using an SPS-825S DR. SINTER apparatus under a vacuum condition (~ 6-8 Pa). A total of 9 samples were sintered using experimental parameters shown in Table 1 with the details. Accordingly different heating rates (50 °C/min and 100 °C/min), sintering temperatures (750 °C, 800 °C, 850 °C, and 900 °C), dwell times (3 mins and 5 mins) and pressures (40 MPa and 80 MPa) were used. The SPS'ed samples were ground and polished to fine and graphite-free surfaces prior to density measurements and microhardness testing.

Table 1. List of SPS'ed samples with corresponding process parameters.

Sample #	Heating Rate (C/min)	Dwell Temp [C]	Dwell Time (mins)	Pressure (MPa)
1	50	750	5	80
2	50	800	5	80
3	50	850	5	80
4	50	900	5	80
5	50	850	3	80
6	50	850	5	40
7	100	850	3	80
8	50	850	3	40
9	100	850	5	40

3.3.3 Microstructural Analysis of SPS'ed CP-Ti

Representatives of SPS processed sample microstructures are given in Figures 16(a)-(d), which is characterized by distinct coarse grained and fine-grained regions, in agreement with bimodal material design (i.e., powder blending). The size distribution of the grains in the fine grained region was measured to be in the range of 150-500 nm, and in the coarse grained region was measured to be in the range of 1000 nm – 3000 nm. Another characteristic of the microstructures is the observed dislocation tangling near grain boundaries as represented in Figure 16(d).

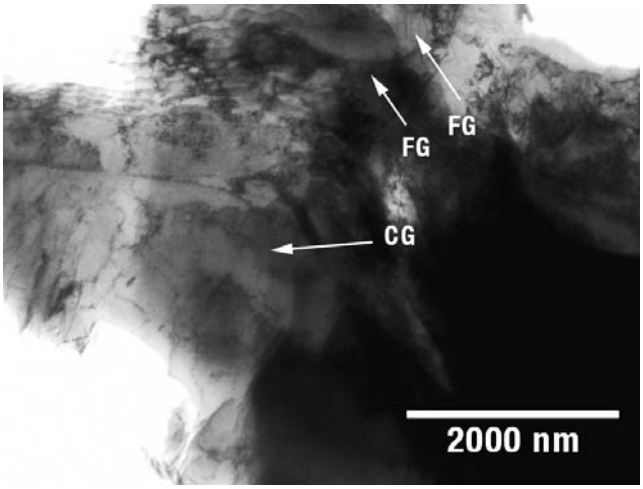

(a)

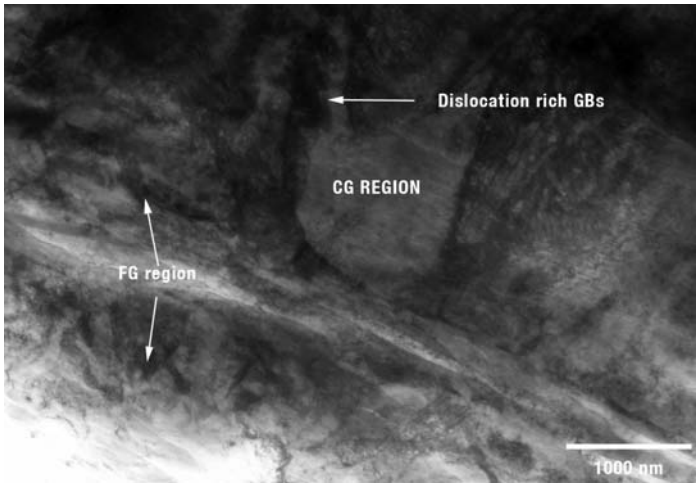

(b)

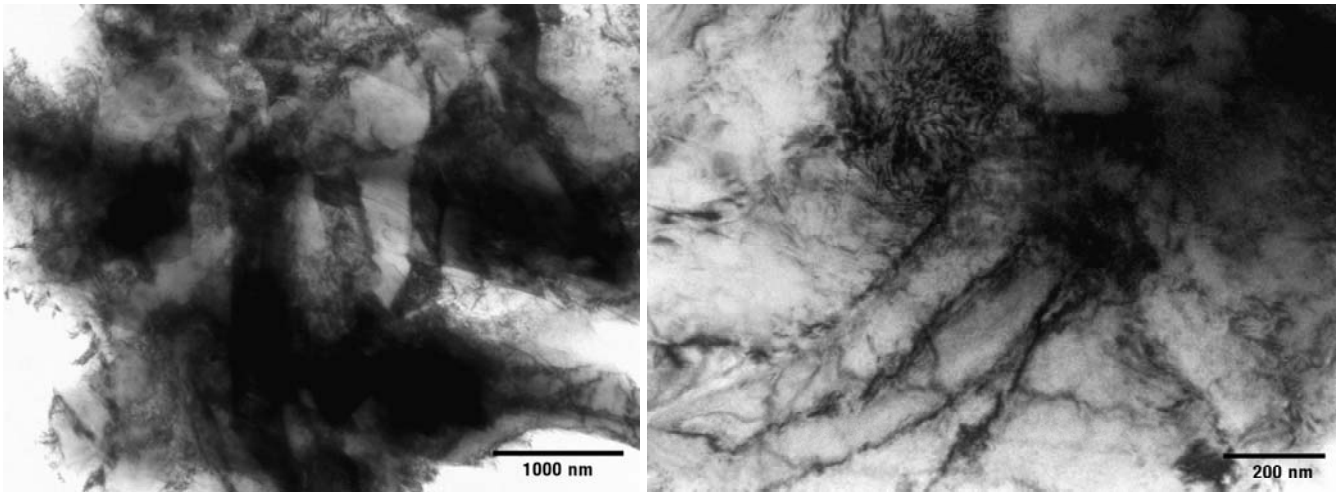

(c) (d)

Figure 16. Representative microstructure images showing: (a) & (b) general view of coarse grained and fine grained regions, (c) fine grained region, and (d) dislocation tangling near grain boundary section.

3.3.4 Mechanical Properties of SPS'ed CP-Ti

Room temperature stress-strain curves for specimens tested at a constant strain rate (10^{-3} s^{-1}) are presented using a comparative approach in Figures 17-20. Samples #1, #2, #3, and #4 are compared in Figure 11, in order to reveal the isolated effect of sintering temperature (i.e., identical heating rate, pressure and dwell time). Very close YS and UTS values were measured for these samples. However, not surprisingly, a higher sintering temperature effectively improved the ductility. Such behavior is attributable to weaker particle-particle interfaces for samples consolidated below 850 °C. Therefore, the high post necking strain measured for #4 is attributable to improved inter-particle bonding that hinders crack propagation through particle boundaries. The retained strength at high temperatures is attributable to limited grain growth at short processing times for SPS.

In Figure 18(a)-(b), the effect of applied pressure was compared for different samples using a similar approach (i.e., identical heating rate, temperature, and dwell time). Not surprisingly, a higher applied pressure (80 MPa) improved the strength and ductility of samples due to the attained higher density.

Again, a similar comparative approach was used for heating rate (i.e., identical pressure, temperature, and dwell time) and dwell time (i.e., identical heating rate, temperature, and pressure) dependence. A lower heating rate of 50 °C/min was found to improve the properties as compared to a higher heating rate, in different ways when different pressures were applied (i.e., higher strength for 40 MPa applied pressure [Figure 19(b)] and higher ductility for 80 MPa applied pressure [Figure 19(a)]). Both sample #6 (50 °C/min) and sample #9 (100 °C/min) processed using a lower applied pressure exhibited a limited post necking strain due to a relatively lower density. The higher strength of #6 is attributable to less localization of heating at lower heating rates reducing the excessive grain growth. However, as explained previously, such localization effects are smaller when a higher applied pressure is utilized. Accordingly, sample #7 (100 °C/min) and #5 (50 °C/min) (80 MPa applied pressure for both) exhibit relatively similar tensile behavior when compared to each other. The larger post necking elongation for #5 is attributable to a longer total processing time improving particle bonding.

A notably higher strength and ductility was observed for sample #5 (3 mins of dwell time) as compared to sample #3 (5 mins of dwell time) revealing the dwell time dependence as illustrated in Figure 20. The longer dwell time is thought to cause coarsening and annihilate the non-equilibrium microstructure (characterized by a high interface energy and randomly oriented dislocations at grain boundaries) due to the thermal recovery effect. The higher strength of cryomilled CP-Ti as compared to that of conventionally processed CP-Ti, is primarily attributable to the following factors: a refined microstructure, an increased interstitial solute concentration, and dislocation strengthening. These factors are not independent from each other, because the microstructure formation, and deformation in hcp Ti has a strong dependence to interstitial solute concentration.

One of the most conspicuous findings in the present study is the measured high ductility. Elongation to failure values ~30% were measured for samples with high strength (e.g., #4 and #5). As mentioned previously, elimination of extrinsic effects such as porosity or insufficient inter-particle bonding is an essential first step. However, even a density near theoretical value and perfect inter-particle bonding does not guarantee a high ductility. The intrinsic microstructure governs the deformation and is responsible for the mechanical response to applied loads. In the present study, formation of a bimodal microstructure attained via blending of as-received coarse grain powders with cryomilled powders, is thought to provide strain hardening and thereby help delay necking instabilities. The introduction of coarse grains into an ultra-fine and/or nano grained matrix, also represents an effective strategy to suppress crack growth and help retain fracture toughness. This is also thought be an additional mechanism for the retained high ductility in SPS cryomilled CP-Ti materials in the present study.

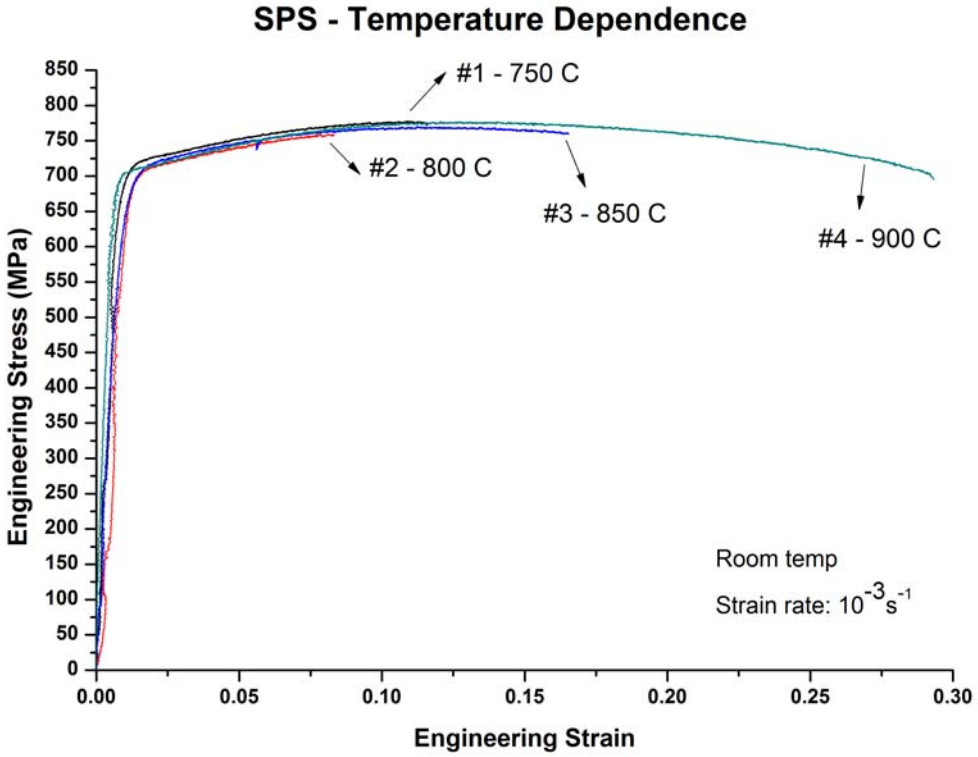

Figure 17. Engineering stress-strain curves comparing #1, #2, #3, and #4, in order to reveal SPS temperature dependence.

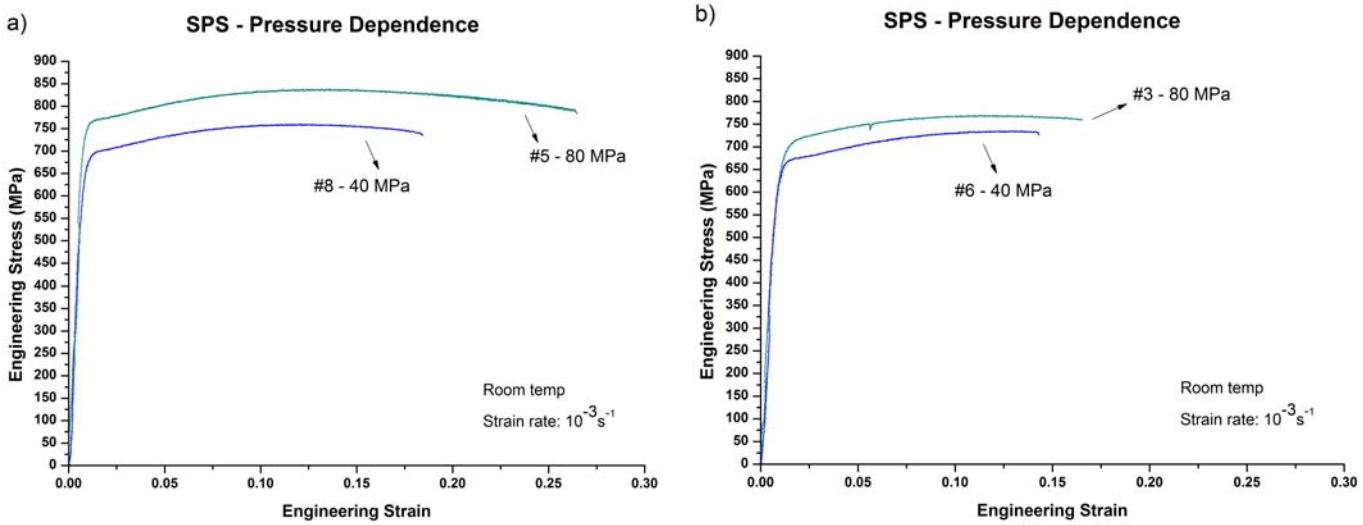

Figure 18. Engineering stress-strain curves comparing a) #5 and #8 (dwell time=5 mins) b) #3 and #6 (dwell time= 3 mins), in order to reveal SPS pressure dependence.

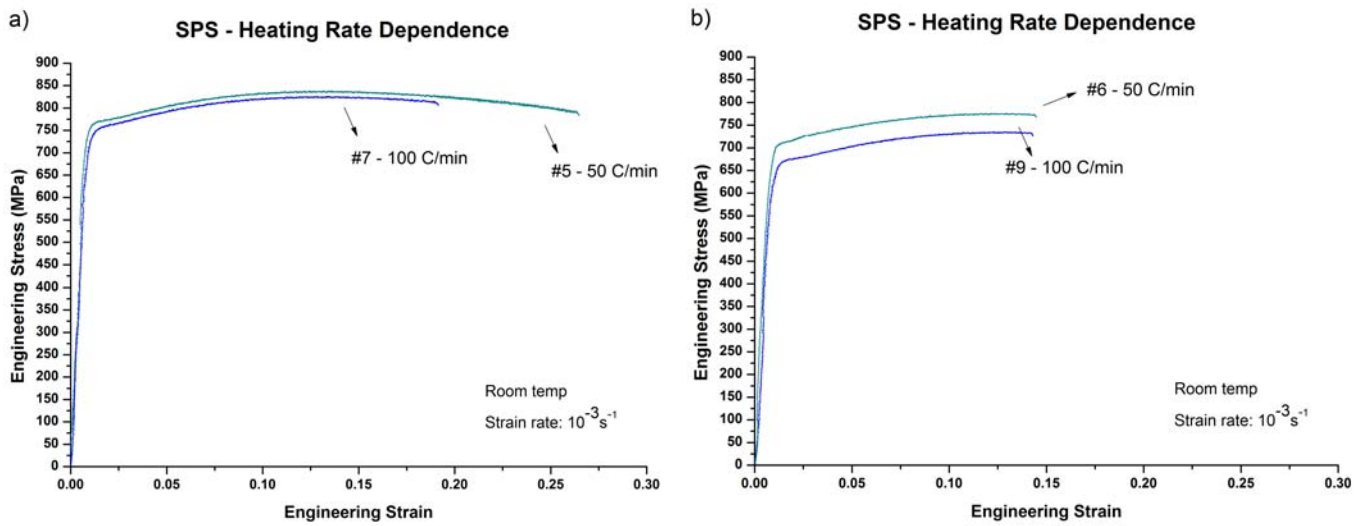

Figure 19. Engineering stress-strain curves comparing a) #5 and #7 (pressure = 80 MPa) b) #6 and #9 (pressure = 40 MPa), in order to reveal SPS pressure dependence.

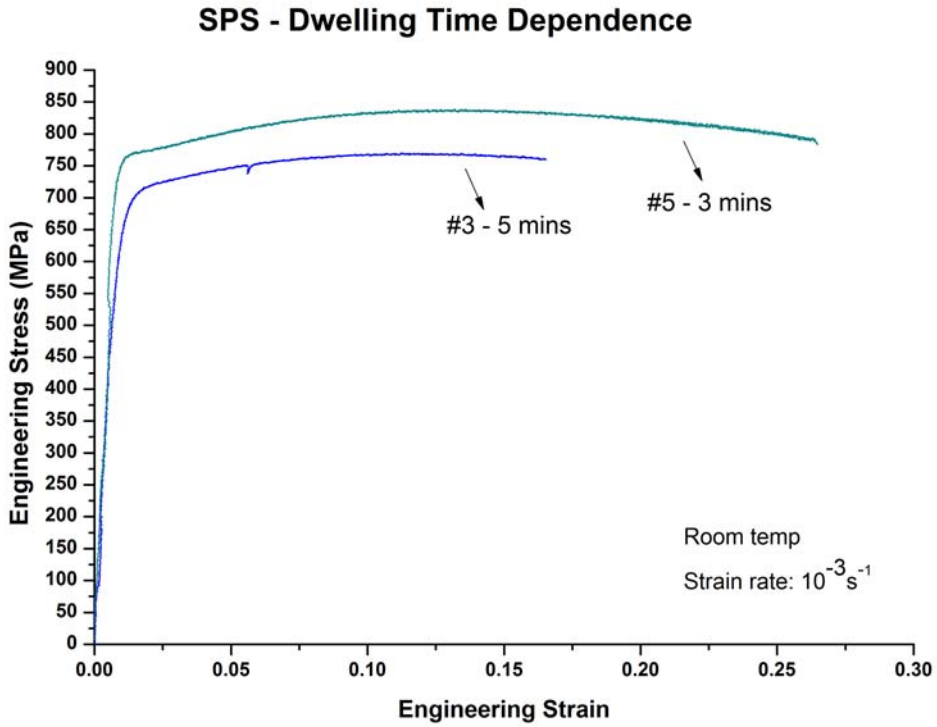

Figure 20. Engineering stress-strain curves comparing #3 and #5 in order to reveal dwell time dependence.